Eur. Phys. J. E (2023) 46:66
https://doi.org/10.1140/epje/s10189-023-00324-4

THE EUROPEAN
PHYSICAL JOURNAL E

Regular Article - Soft Matter

Impact of flexibility on the aggregation of polymeric macromolecules

Soheila Emamyari[1], Masoud Mirzaei[1], Sarah Mohammadinejad[2], Davood Fazli[1], and Hossein Fazli[1,2,a]

[1] Department of Physics, Institute for Advanced Studies in Basic Sciences (IASBS), Prof. Yousef Sobouti Blvd., Zanjan 45137-66731, Iran
[2] Department of Biological Sciences, Institute for Advanced Studies in Basic Sciences (IASBS), Prof. Yousef Sobouti Blvd., Zanjan 45137-66731, Iran

Received 12 May 2023 / Accepted 17 July 2023 / Published online 31 July 2023

Abstract Dependence of the dimerization probability and the aggregation behavior of polymeric macromolecules on their flexibility is studied using Langevin dynamics simulations. It is found that the dimerization probability is a non-monotonic function of the polymers persistence length. For a given value of inter-polymer attraction strength, semiflexible polymers have lower dimerization probability relative to flexible and rigid polymers of the same length. The threshold temperature of the formation of aggregates in a many-polymer system and its dependence on the polymers persistence length is also investigated. The simulation results of two- and many-polymer systems are in good agreement and show how the amount of flexibility affects the dimerization and the aggregation behaviors of polymeric macromolecules.

1 Introduction

Phase separation, self-assembly and aggregation of macromolecules under a variety of conditions driven by non-covalent interactions is ubiquitous in nature [1–5]. Among different macromolecules, desired and undesired aspects of the phase separation, the self-assembly and the aggregation of biological polymers such as proteins and peptides, has strongly attracted the scientists attention in the recent years [6–35]. Surface engineering, scaffolding for tissue repair and fabrication of conducting nanowires are some potential applications of the macromolecular self-assemblies [36–44]. Aggregation of macromolecules, especially in biology, is not always desirable. For example, aberrant aggregation of proteins and peptides can lead to a number of diseases such as Alzheimer's disease, Parkinson's disease and type II diabetes [45–51]. Liquid-liquid phase separation of proteins containing disordered regions has been shown that is crucially important for the cell in order to form liquid-like and dissolvable membraneless organelles [15–35]. Nevertheless, it has also been observed that liquid droplets of protein condensates are prone of aberrant aggregation, solidification and maturation into fibrilar protein assemblies [15,18–23,28]. Surface modification is another important issue in which short polymeric chains of amino acids (polypeptides) has been widely used to improve the compatibility of given materials with other materials or environments. For example, the evidence that an ionic-complementary peptide, EAK16-II, is capable of assembling on hydrophilic mica as well as hydrophobic highly ordered pyrolytic graphite (HOPG) surfaces with different nano-patterns [52] has been presented.

In a solution of macromolecules, parameters such as inter- and intra-molecular interactions, properties of the solvent and architecture of the molecules can affect the system behavior. The presence of other objects such as an interacting surface can also affect the aggregation behavior of the macromolecules considerably [53]. The interaction of peptides and proteins with various surfaces and formation of nanostructures has been investigated [54–59]. These nanostructures can be useful in devices such as biosensors and information storage units [60,61].

Most of the amazing behaviors of polymeric macromolecules are due to their polymeric nature and do not depend on their details in atomic level. Accordingly, one can study the behavior of such macromolecules using simple coarse-grained models and generalize the results to a wide category of biological and synthetic polymers. In a dilute solution of polymeric macromolecules, dimerization is very early and an important stage of the aggregation process. On the other hand, study of a two-polymer system in detail is quite feasible using simulation methods. Accordingly, a systematic and detailed study of the dimerization process can be helpful in description of the aggregation behavior of many-polymer systems. Decreasing the number of accessible configurations of two polymers undergo-

---

[a] e-mail: fazli@iasbs.ac.ir (corresponding author)

ing dimerization leads to an effective reduction of their entropy which is equivalent to the polymers unwillingness to aggregate. The amount of the entropy decrease in the course of aggregation depends on the polymers structural properties such as their flexibility. On the other hand, dimerization of two polymers that attract each other, lowers the system internal energy and the total change of the system free energy determines the probability of dimerization. The study of the entropic unwillingness and generally the probability of dimerization can help to understand the behavior of polymers in a dilute solution and in the nucleation step of the aggregation.

Flexibility of a polymeric macromolecule (which can be quantified by the value of its persistence length [62]), depends on chemical bonds along its backbone as well as the spacial structure and architecture of the molecule (such as presence or absence as well as the size of side chains). For example, in the case of peptides and proteins, the amount of the chain flexibility depends directly on the amino acid sequence of the macromolecule. In this case, presence of amino acids such as glycine increases the chain flexibility, however, amino acids like proline cause the chain to be less flexible [63].

In this paper, we study the effect of the polymer chains flexibility on their aggregation behavior using Langevin dynamics (LD) simulations. The model polymers in our study are considered to be homopolymers for simplicity. This assumption enables us to concentrate solely on the role of polymer flexibility. However, real biological polymers are mostly heteropolymers and variety of interactions between different monomers have crucial role on their rich phase behavior. Some effects of heterogeneity on the phase separation of disordered proteins have recently been studied [64]. It is worth to mention amount of the flexibility of proteins (or polypeptides) depends on the hierarchy of their folding which originates from the amino acid sequence. Disordered parts of proteins are more flexible than the folded parts. Regarding the dimensionless nature of quantities in LD simulations, the obtained results in our study can shed light on the effect of flexibility on the aggregation of polymeric macromolecules in a range of length scales. To study the impact of biopolymers flexibility on their aggregation behavior, we first measure the probability of dimerization in a system containing two polymers that weakly attract each other and study dependence of the probability on the polymers persistence length. We find that keeping the strength of attraction between the polymers fixed, the dimerization probability is a nonmonotonic function of the polymers persistence length. For a given value of the attraction strength, semiflexible polymers show lower dimerization probability relative to flexible and rigid polymers of the same contour length. Then, we study the effect of the polymers persistence length on their aggregation behavior by simulation of a many-polymer system. We obtain the threshold temperature for the formation of stable aggregates in these simulations and it is found that the threshold temperature has also a nonmonotonic dependence on the polymers flexibility. The results of the two sets of simulations are in good agreement.

The rest of the paper is organized as follows. We introduce the model and the details of our simulations in Sect. 2. The results and discussions are presented in Sect. 3. The paper is concluded in Sect. 4.

2 The model and the simulation method

We use coarse-grained, bead-spring model polymers in our Langevin dynamics (LD) simulations. Each polymer in our simulations consists of $N = 16$ monomers. Non-bonded interactions between the monomers of a polymer with the monomors of the other polymers (inter-polymer interactions) are modelled by Lennard–Jones potential;

$$U_{\mathrm{LJ}}(r) = \begin{cases} 4\varepsilon_0[(\frac{\sigma}{r})^{12} - (\frac{\sigma}{r})^6] & r \leq 3.5\sigma, \\ 0 & r > 3.5\sigma, \end{cases} \tag{1}$$

where σ is the monomer diameter and the LD length scale and ε_0 is the Lennard–Jones energy scale. The interactions between the monomers of a polymer (intra-polymer interactions) are also modeled by Lennard–Jones repulsive potential (hard-core repulsion):

$$U_{\mathrm{LJ-rep}}(r) = \begin{cases} 4\varepsilon_0\left[(\frac{\sigma}{r})^{12} - (\frac{\sigma}{r})^6 + \frac{1}{4}\right] & r \leq 2^{1/6}\sigma, \\ 0 & r > 2^{1/6}\sigma, \end{cases} \tag{2}$$

Consecutive monomers of each polymer are connected by a harmonic potential, $U_\mathrm{h} = 1/2k_\mathrm{h}(r - R)^2$, with spring constant and equilibrium distance between connected monomers of $k_\mathrm{h} = 90k_\mathrm{B}T$ and $R = 1.1\sigma$, respectively. Bending rigidity of each polymer chain is modelled by a bond angle potential between two successive bonds connecting three successive monomers, defined as

$$U_{\mathrm{bend}} = k_{\mathrm{bend}}(1 - \cos(\theta - \theta_0)), \tag{3}$$

where k_{bend} is the bending constant, θ is the angle and θ_0 is the equilibrium angle between two successive bonds. The equilibrium angle in our simulations is zero and the bending constant is $l_\mathrm{p}k_\mathrm{B}T$, in which l_p is the persistence length of the polymer chain.

Simulations are carried out with the MD simulation package ESPResSo (version 4) [65] (dimerization simulations) and with LAMMPS [66] (aggregation of many polymers). All simulations are performed in $60\sigma \times 60\sigma \times 60\sigma$ cubic box and periodic boundary conditions in three dimensions are applied.

The time step of the simulations is $\tau = 0.01\tau_0$, where $\tau_0 = \sqrt{m\sigma^2/\varepsilon_0}$ is the MD time scale, and m is the monomer mass. The simulations are carried out in the NVT ensemble using the Langevin thermostat. The dimerization simulations are performed at fixed temperature $T = 1.0\varepsilon_0/k_\mathrm{B}$ and the polymers aggregation simulations are performed at different temperatures (all temperatures are in units of $\varepsilon_0/k_\mathrm{B}$). The Langevin equation, $m\ddot{\vec{r}} = -\xi_\mathrm{b}\dot{\vec{r}} + \vec{F}_\mathrm{ext} + \vec{\eta}(t)$, is integrated for finding the positions of the monomers at each time step. In this equation, ξ_b is the friction coefficient and $\vec{F}_\mathrm{ext}$ is the external force exerted from the other particles. $\vec{\eta}(t)$ is also a random force, which obeys the fluctuation-dissipation theorem. The reduced friction coefficient in our simulations is 1.

2.1 Dimerization of two polymer chains

We use 'dimerization' term to separate the aggregation in the level of a two-polymer system from that in the level of a many-polymer system in our study. One should note regarding the coarse-grained nature of our simulations that no specific binding between the polymers is defined and dimerization can not have further meaning than aggregation here.In the beginning of the simulation study of the dimerization process, we construct two polymers in the extended conformation and parallel to each other in the simulation box, with the initial separation of d_ini, such that the center of mass of the polymers is in the middle of the simulation box. Then, we let the polymers to equilibrate for 10^6 time steps. After that, the main simulation is performed for $N_\mathrm{t} = 6 \times 10^8$ time steps. In each time step, if the LJ energy between the two polymers is lower than $(N/2)k_\mathrm{B}T$ (in which almost half of the monomers of a polymer are in contact with the other polymer), they are assumed to be aggregated. The probability of aggregation is the ratio of the number of time steps in which two polymers are aggregated (n_agg) to the total number of the simulation time steps (N_t):

$$P_\mathrm{agg} = \frac{n_\mathrm{agg}}{N_\mathrm{t}}. \tag{4}$$

Also, every 6×10^5 time steps a configuration of the system is saved for analyzing the average of LJ interaction energy of the two polymers over time.

2.2 Aggregation of many polymers

To study the aggregation of many polymers, we perform simulations with $N_p = 313$ polymers. In the beginning of each simulation, we distribute N_p polymers in the simulation box randomly in a way that there is no overlap between them. Then, we run the system in NVT ensemble for 5×10^6 time steps and study the aggregation behavior of the polymers. Simulations are performed at different temperatures, ranged from 1.5 to 3.5, to study temperature-dependence of the aggregation process for polymers of different persistence lengths. By performing simulations at different temperatures, the threshold temperature for aggregation below which a stable aggregate forms and above that a dilute solution of the polymers coexists with the aggregate can is found.

3 Results and discussion

3.1 Dimerization

Two similar polymers with the initial separation of $d_{ini} = 4\sigma$ in three dimensional bulk are simulated (the polymers are initially parallel to each other). With such a small value of d_{ini}, we eliminate the diffusion step of the aggregation process which is not of our interest in this study. Omission of the diffusion stage can also be archived by doing the simulation in a smaller simulation box keeping periodic boundary conditions. We found no difference in our results using both methods. Figure 1 shows the dependence of the dimerization probability on the ratio of polymers persistence length to their contour length (l_p/L). As it can be seen, the dimerization probability versus l_p/L is a non-monotonic function. It decreases from $l_\mathrm{p} = 0$ to $l_\mathrm{p}/L = 0.44$, and then increases. The flexible and the rod-like polymers have larger dimerization probability compared with the semiflexible ones. Sample snapshots of the dimers of flexible ($l_\mathrm{p} = 0$), semiflexible ($l_\mathrm{p}/L = 0.44$) and rod-like ($l_\mathrm{p}/L = 5.63$) polymers are also shown in Fig. 1. The monomers of the flexible polymers attract each other and an aggregate composed of the monomers of the two polymers forms. The polymers become more extended by increasing the persistence length and finally, at large persistence lengths, the two polymers dimerize as two

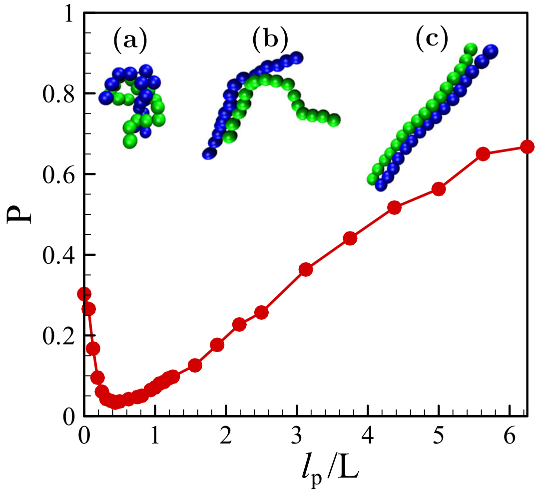

Fig. 1 Dimerization probability versus the ratio of polymers persistence length to their contour length. Sample snapshots of the polymers (shown in blue and green) are also illustrated for flexible ($l_\mathrm{p} = 0$) (**a**), semiflexible ($l_\mathrm{p}/L = 0.44$) (**b**) and rod-like ($l_\mathrm{p}/L = 5.63$) (**c**) polymers. Dimerization probability is a non-monotonic function of the polymers persistence length. The solid line connecting the data points is only a guide for eye. Error bars on the data points are at most as large as the symbol size

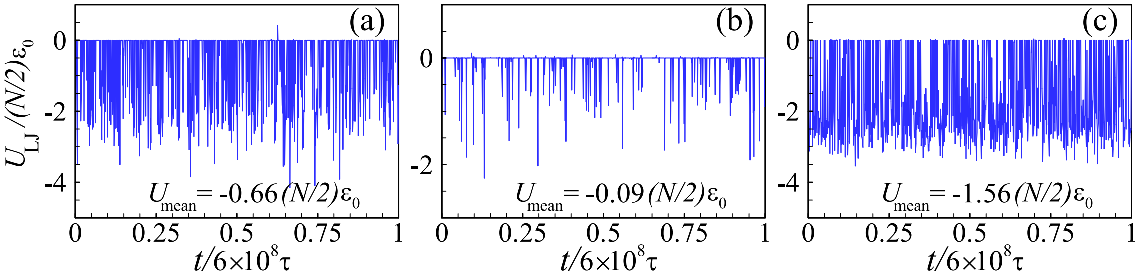

Fig. 2 Dimensionless LJ interaction energy of the two polymers undergoing dimerization versus time in simulations of flexible ($l_p = 0$) (**a**), semiflexible ($l_p/L = 0.44$) (**b**) and rod-like ($l_p/L = 5.63$) (**c**) polymers. Time average of the interaction energies are shown on the figure panels

rods (see the snapshot of $l_p/L = 5.63$ in Fig. 1). Also, the error bars of the obtained data in these figures, which are resulted from averaging over 10 runs of the simulation, are at most as large as the symbol size.

Both the entropic effects which have a deterrent effect against the dimerization and the effect of attraction potential should be considered to explain the dimerization behavior of the two polymers. The entropy of a polymer chain is related to the number of its possible configurations. If Ω is the number of configurations of a monomer relative to the previous monomer along the polymer chain, and N is the number of monomers of the polymer, the entropy of the polymer (S) can be written as

$$S = Nk_{rmB} \ln \Omega \tag{5}$$

The number of possible configurations of each monomer relative to the previous one decreases (and hence the entropy of the polymer chain decreases) by increasing the polymer bending rigidity. The free energy of the system of two polymers can be written as

$$F = U - TS, \tag{6}$$

in which, U is the attraction energy between the polymers. Since we are interested in the dimerization probability of the polymers, we focus on inter-polymer LJ energy (shown by U_{LJ}) and its average over time (shown by U_{mean}).

Figure 2 shows the time evolution of $\frac{U_{\mathrm{LJ}}}{(N/2)\varepsilon_0}$ for flexible ($l_p = 0$), semiflexible ($l_p/L = 0.44$) and rod-like ($l_p/L = 5.63$) polymers. Time average of the interaction energy, U_{mean}, is also calculated and shown in the inset of the figures. Anytime $\frac{U_{\mathrm{LJ}}}{(N/2)\varepsilon_0}$ is less than -1, one can roughly say at least half of the monomers of a polymer are in contact with the other polymer. Also, the longer time the polymers are aggregated, the lower the amount of U_{mean}. Two flexible polymers can undergo dimerization process without significant loss of their conformational entropy. One should note that a dimer formed by two flexible polymers is itself a flexible object of entropy as high as a flexible polymer. The energy of the system also decreases (to $U_{\mathrm{mean}} = -0.66(N/2)\varepsilon_0$) as the two flexible chains form a dimer (see Fig. 2 for $l_p = 0$). Hence, the dimerization can take place and the probability of dimerization has a noticeable value ($\simeq 0.3$, see Fig. 1 for $l_p = 0$).

By increasing the persistence length, the dimerization probability decreases and reaches a minimum value for semiflexible polymers of $l_p/L = 0.44$. In this case, the two polymers are not able to aggregate and decrease the LJ energy to the extent that the flexible polymers do. As presented in Fig. 2, $U_{\mathrm{mean}} = -0.09(N/2)\varepsilon_0$ is obtained for $l_p/L = 0.44$ which is considerably larger than $U_{\mathrm{mean}} = -0.66(N/2)\varepsilon_0$ for $l_p = 0$. For two semiflexible polymers, the entropy of two single chains are still significant and they have to lose their entropy substantially in the course of dimerization ($\Delta S < 0$). In this case, one should note that an aggregate of two semiflexible polymers is an object of lower flexibility and hence of lower entropy. As a result, the aggregation process becomes difficult for semiflexible polymers and the value of dimerization probability is smaller relative to the case of flexible polymers.

By further increasing the polymers persistence length, we study the dimerization process of two rod-like polymers to measure the dimerization probability. The thermal energy is not able to bend rod-like polymers and to activate their internal degrees of freedom. Such polymer have small entropy and their aggregation does not decrease the entropy of the system considerably ($\Delta S \simeq 0$). On the other hand, the aggregation leads to larger decrease of LJ energy ($U_{\mathrm{mean}} = -1.56(N/2)\varepsilon_0$) relative to the flexible and semiflexible polymers (see Fig. 2). Thus, the aggregation becomes easier and the dimerization probability increases.

As mentioned above, the entropy loss of two semiflexible polymers in the course of dimerization is noticeable, while in the case of two flexible or rod-like polymers, there is no much difference in entropy of the two polymers when they are dissolved or aggregated as a dimer. Therefore, semiflexible polymers have a less dimerization probability compared to flexible and rod-like polymers. The increase in free energy due to the decrease in entropy can be compensated by strengthening the attraction between the two semiflexible polymers. In this way, the dimerization probability of the two polymers increases.

As it can be seen in Fig. 1, for two values of the polymer flexibility ($l_p/L = 0.06$ and 2.5) dimerization probabilities are the same (approximately 0.25) and noticeably larger than that for semiflexible polymers

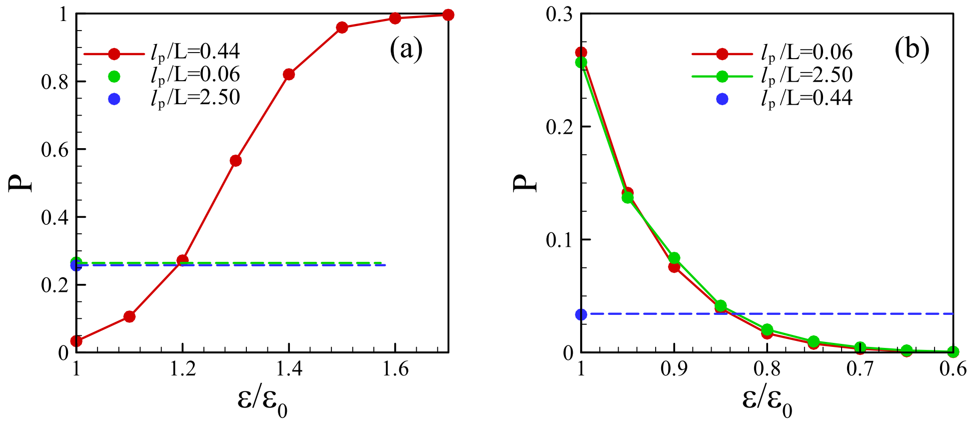

Fig. 3 Comparison of the dimerization probability of flexible and rod-like polymers at attraction strength $\varepsilon/\varepsilon_0 = 1$ between the monomers with that of semiflexible polymers at different values of $\varepsilon/\varepsilon_0$ (**a**). Comparison of the dimerization probability of semiflexible polymers at $\varepsilon/\varepsilon_0 = 1$ with those of flexible and rod-like polymers at different values of $\varepsilon/\varepsilon_0$ (**b**) (see the text)

of $l_\mathrm{p}/L = 0.44$. A question that arises here is about the value of attraction strength $(\varepsilon/\varepsilon_0)$ between two semiflexible polymers of $l_\mathrm{p}/L = 0.44$ needed to overcome their excess unwillingness for dimerization. To this end, dimerization probability of two semiflexible polymers at different values of the attraction strength, $\varepsilon/\varepsilon_0$, is shown in Fig. 3a. The values of dimerization probability for couples of polymers with $l_\mathrm{p}/L = 0.06$ and 2.5 at $\varepsilon/\varepsilon_0 = 1$ are also shown in this figure for comparison. Dashed lines are guides for eye and shows the value of $\varepsilon/\varepsilon_0$ for which dimerization probability for couples of polymers with three different values of flexibilities is the same. The fact that the probabilities are the same at $\varepsilon/\varepsilon_0 = 1.2$ shows that 20 percent stronger attraction between the polymers is needed to overcome semiflexible polymers more unwillingness for dimerization relative to flexible and stiff polymers. The other way above mentioned question can be asked is how much the attraction strength for couples of flexible and stiff polymers should be decreased to obtain equal dimerization probabilities for couples of polymers with three above mentioned flexibilities. To this end, aggregation probabilities are shown for couples of flexible and stiff polymers versus $\varepsilon/\varepsilon_0$ in 3b and compared with that of semiflexible polymer at $\varepsilon/\varepsilon_0 = 1$. As it can be seen, by decreasing the attraction strength of flexible and stiff polymers to $\varepsilon/\varepsilon_0 = 0.84$ the dimerization probabilities for couples of polymers with three different values of flexibility become the same.

To investigate the effect of intramolecular attractions on the dimerization probability, we perform simulations in which the repulsive Lennard–Jones interaction between the monomers of each polymer in Eq. 2 has been replaced by the Lennard–Jones interaction of Eq. 1. In this way, there is an attractive interaction between all monomers in the system. The dependence of dimerization probability on the persistence length is investigated in this condition and the results are shown in Fig. 4. This figure shows that the intramolecular attractions affect the dependence of dimerization probability on the polymers flexibility only for polymers with $l_\mathrm{p}/L \leq 0.125$ relative to the case without intramolecular attractions shown in Fig. 1. As it is shown in the inset of Fig. 4, the dimerization probability increases slightly as the persistence length increases from 0 to $0.125L$. To describe this behavior one should note that a fully flexible polymer in a poor solvent collapses and forms a dense globule made of monomers. As two such collapsed polymers meat each other in the solution, only a few monomers on their surface can interact with each other (imagine two spheres touching each other). Such a weak interaction between the two globular polymers is not strong enough against thermal fluctuations to keep the polymers together. By a slight increasing of the persistence length from zero to $l_\mathrm{p}/L = 0.125$, dense globular conformation of the polymers opens and a higher number of their monomers can interact with each other. Hence, inter-polymer interaction becomes stronger in competition with thermal fluctuations and the dimerization probability increases up to $l_\mathrm{p}/L = 0.125$. By further increasing the persistence length, the effect of intramolecular attractions becomes negligible, and the dimerization probability shows almost the same behavior as the case wihtout intramolecular attractions shown in Fig. 1.

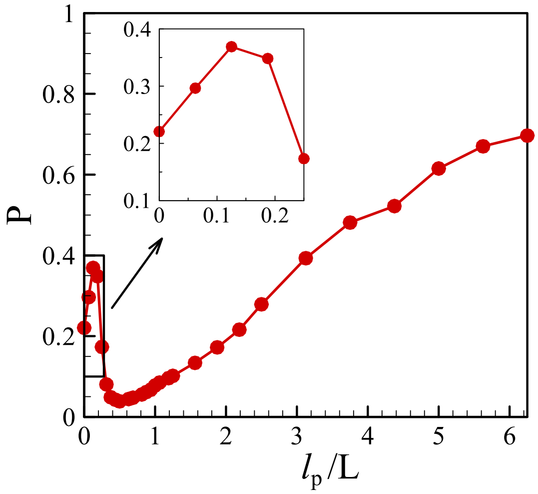

Fig. 4 Dimerization probability versus the ratio of polymers persistence length to their contour length for two polymers free in space, by considering the intramolecular attraction force between monomers of a polymer

One should note the above mentioned result is in the case of a two-polymer system. In a solution of many polymers, depending on the order of magnitudes of the time scales associated with internal relaxation of single polymers on one hand and the diffusion of polymers to find each other in the aggregation process on the other hand, different scenarios such as entangled or disentangled aggregations may occur [67].

It is worth to mention that we rechecked the probability of dimerization at different values of the polymers persistence length by changing dimerization criteria from inter-polymer LJ energy to the neighborhood matrix for the monomers from the two polymers and obtained the same results. We also checked by changing the amount of LJ energy between the polymers below which they are considered as aggregated ($(N/2)k_BT$ in our study) and found that the results are mostly the same.

3.2 Aggregation in many-polymer system

As described in Sect. 2, simulations at different temperatures are performed for 5×10^6 time steps to find the threshold temperature for aggregation (T^*) and its dependence on the persistence length of the polymers. It should be noted that 5×10^6 time steps is enough for the systems to reach equilibrium and take its stable state in all of the simulations. At temperatures below T^* aggregate of the polymers forms and at temperatures slightly above T^* a dilute solution of polymers and an aggregate coexist in the system. Indeed, T^* for each system is the lowest temperature at which some polymer chains tend to leave the aggregate.

The resulting threshold temperatures for polymers of different persistence lengths, ranged from $l_p/L = 0$ (flexible polymer) to $l_p/L = 5.63$ (rod-like polymer), are shown in Fig. 5. Error bars of the obtained data in this figure are of the order of 0.1 which are not shown in the figure for clarity. As this figure shows, the polymer chains flexibility affects the aggregation threshold in many-polymer level very similar to the dimerization process as discussed above. It is found that the threshold temperature for aggregation of semiflexible polymers with $l_p/L = 0.44$ is lower than those of flexible and rod-like polymers. It means that, if we have three clusters of flexible, semiflexible and rod-like polymers at low temperature, as the temperature increases, the aggregate of semiflexible polymers starts to dissolve earlier compared to flexible and rod-like polymers.

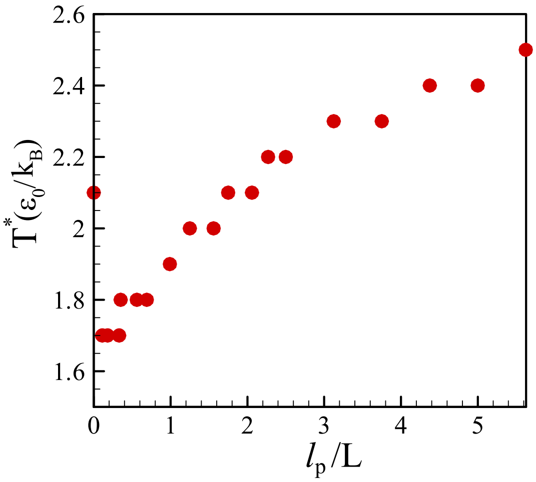

Fig. 5 Threshold temperature for aggregation of polymers versus the ratio of polymers persistence length to their contour length

Some snapshots of the final aggregations of the polymers in the simulation box for flexible ($l_\mathrm{p} = 0$), semiflexible ($l_\mathrm{p}/L = 0.44$) and rod-like ($l_\mathrm{p}/L = 5.63$) polymers are shown in Fig. 6, at temperatures $T = 2.0$ (below the threshold temperature for flexible polymers), $T = 2.2$ (above the mentioned threshold) and $T^* = 2.1$ (the threshold temperature for flexible polymers). As it is shown in this figure, at the given temperature, $T = 2.0$, all of the flexible and rod-like polymers are aggregated in a single bundle (see Fig. 6(a_1) and (c_1)). However, at the same temperature, in the system of semiflexible polymers an equilibrium between an aggregate and single polymers dispersed in the solution can be observed (see Fig. 6(b_1)). To form a single aggregate in the system of semiflexible polymers similar to the systems of flexible and rod-like polymers, one has to lower the temperature by at least 20 percent until it reaches $T = 1.6$ (as it can be found in Fig. 5). So, at both temperatures ($T = 2.0$ and $T = 2.2$) a dense aggregate and single polymers dispersed in the solution coexist for the system of semiflexible polymers (see Fig. 6(b_1) and (b_2)). At higher temperatures, more single polymers are dispersed in the solution and the dense aggregate is smaller. In the case of rod-like polymers a single aggregate forms at both temperatures, since the threshold temperature of rod-like polymers is higher than 2.2 ($T^* = 2.5$ for rod-like polymers as it can be seen in Fig. 5). On the other hand, $T = 2.2$ is slightly higher than the threshold temperature of flexible polymers and as it can be seen in Fig. 6(a_2), few polymers are dispersed in the solution.

The point to note is that our study here is in the level of polymer aggregation, not phase separation. The number of polymers we considered in many polymer simulations of our study is too small to investigate phase separation phenomenon quantitatively and obtain the system phase diagram. As mentioned above, our study here is concentrated on the impact of polymer chains flexibility in two- and many-polymer levels (a bottom up approach). There are well known simulation techniques in the literature for quantitative study of polymer phase separation [68]. However, the threshold temperature for polymer aggregation in our study is not too much different from the critical temperature obtained in simulations with large number of polymers with slab geometry of the simulation box [68]. On the other hand, phase separation temperature for a solution of homopolymers can be calculated using mean field approach (Flory-Huggins solution theory) [62]. To this end, the interaction parameter, χ, and the length (number of monomers) of each polymer should be known to

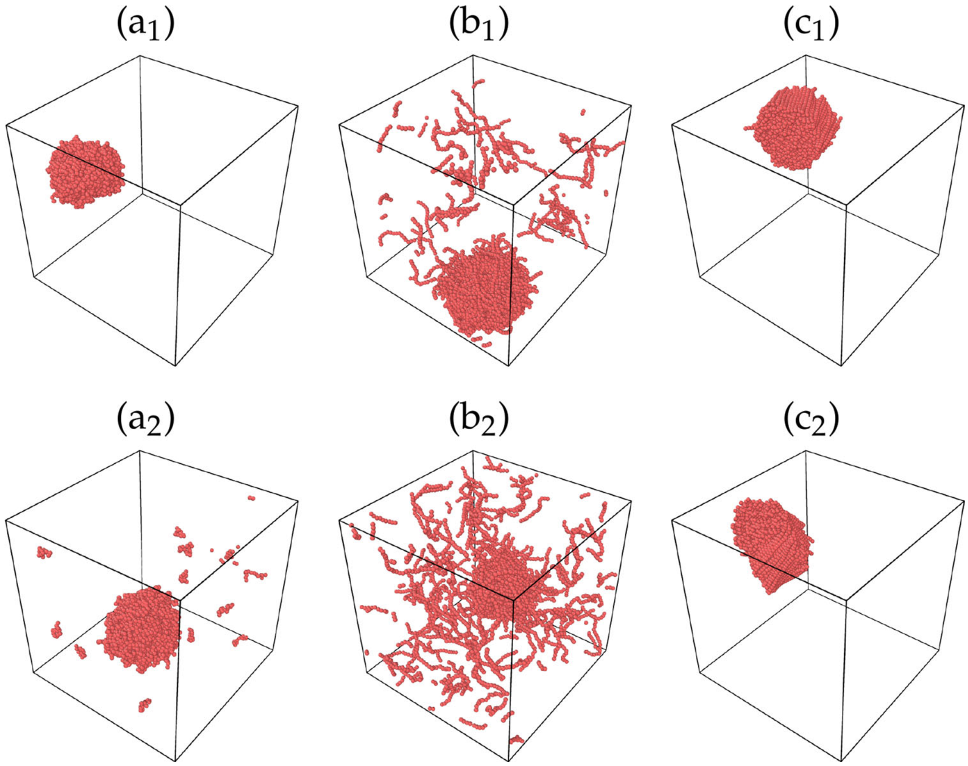

Fig. 6 Snapshots of the final aggregations of the polymers in the simulation box for flexible ($l_\mathrm{p} = 0$) (a_1,a_2), semiflexible ($l_\mathrm{p}/L = 0.44$) (b_1,b_2) and rod-like ($l_\mathrm{p}/L = 5.63$) (c_1,c_2) polymers, at temperature $T = 2$ (a_1,b_1,c_1) and $T = 2.2$ (a_2,b_2,c_2)

use in the Flory-Huggins free energy of mixing [62]:

$$\overline{\Delta F}_\mathrm{mix} = k_B T[\frac{\phi}{N}\ln(\phi)+(1-\phi)\ln(1-\phi)+\chi\phi(1-\phi)] \quad (7)$$

in which, ϕ is the volume fraction of the polymer in the solution. In our study, $N = 16$ and the value of χ at each temperature can be obtained using its relation with excluded volume, v, which depends on monomer-monomer interaction potential of Eq. 1 as

$$v = \int (1 - exp[-U_{LJ}(r)/k_B T])d^3r. \quad (8)$$

The relation between the interaction parameter and the excluded volume reads $v = (1 - 2\chi)\sigma^3$ [62]. In Fig. 7, $\overline{\Delta F}_\mathrm{mix}$ versus ϕ is shown for different values of temperature, T. As it can be seen, $T^* \simeq 2.1$ is a threshold value above which the curves are convex at all values of ϕ and below that a concave part appears in the curve. This value for critical temperature obtained from Flory-Huggins mean field theory is not far from the threshold temperature obtained in our simulations.

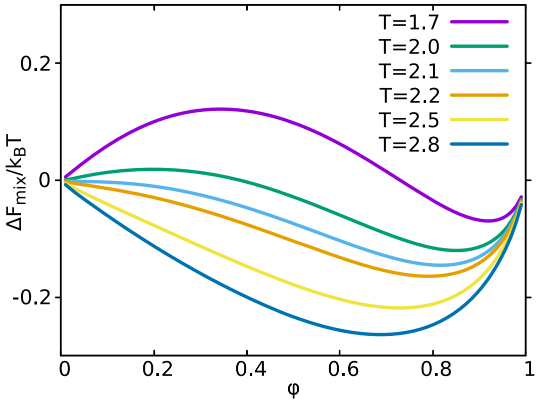

Fig. 7 Dependence of dimensionless free energy of mixing (Flory-Huggins theory) on the polymer volume fraction for a solution of polymers of length $N = 16$ at different values of temperature, T. As it can be seen, at temperature of about 2.1 the shape of the curve changes from fully convex at higher temperatures to a combination of convex and concave parts at lower temperatures shoing that $T^* \simeq 2.1$ in our study is a reasonable value

4 Conclusion

In conclusion, dependence of dimerization probability and aggregation behavior of coarse-grained bead-spring model polymers on their flexibility has been studied using Langevin dynamics simulations. Dimerization probability is a measure of the polymers tendency for aggregation in a dilute solution. Our results showed that the dimerization probability noticeably depends on the value of the polymers persistence length. At a given value of the attraction strength between the polymers, the flexible and the stiff rod-shaped polymers have higher tendency for dimerization relative to semiflexible polymers. Negligible loss of entropy in the course of dimerization for flexible polymers and very low entropy of rigid polymers before and after dimerization are the main origins of higher dimerization probability in these cases relative to the case of semiflexible polymers. One should note that two semiflexible polymers have to lose a noticeable amount of entropy in the course of dimerization (a dimer of two semiflexible polymer is a rigid object of noticeably lower entropy).

To investigate the impact of the polymers flexibility on their aggregation behaviour, we simulated many-polymer systems at different temperatures for polymers of different persistence length. Our results showed that in agreement with the results of dimerization simulations, the aggregation behaviour depends on the polymers flexibility. The threshold temperature, below which a stable aggregate forms (slightly above this threshold dilute solution of polymers and an aggregate coexist in the system), varies with the value of polymers persistence length. It means for example that one can find a value of temperature for which if the polymers are stiff the solution is in aggregated state, but, if the polymers are semiflexible, the solution is mostly in dispersed state.

Soheila Emamyari, Hossein Fazli and Sarah Mohammadinejad contributed to conceptualization and design of the study and preparation of the first draft. Soheila Emamyari, Davood Fazli and Masoud Mirzaei performed simulations. All authors commented on the manuscript and contributed on data interpretation.

Data sets generated during the current study are available from the corresponding author on reasonable request.

References

1. G.M. Whitesides, J.P. Mathias, C.T. Seto, Molecular self-assembly and nanochemistry: a chemical strategy for the synthesis of nanostructures. Science **254**, 1312–1319 (1991). https://doi.org/10.1126/science.1962191
2. G.M. Whitesides, B. Grzybowski, Self-assembly at all scales. Science **295**, 2418–2421 (2002). https://doi.org/10.1126/science.1070821
3. G.M. Whitesides, M. Boncheva, Beyond molecules: self-assembly of mesoscopic and macroscopic components. Proc. Natl. Acad. Sci. U.S.A. **99**, 4769–4774 (2002). https://doi.org/10.1073/pnas.082065899
4. M. Rubenstein, A. Cornejo, R. Nagpal, Programmable self-assembly in a thousand-robot swarm. Science **345**, 795–799 (2014). https://doi.org/10.1126/science.1254295
5. J. Wang, K. Liu, R. Xing, X. Yan, Peptide self-assembly: thermodynamics and kinetics. Chem. Soc. Rev. **45**, 5589–5604 (2016). https://doi.org/10.1039/C6CS00176A
6. S. Zhang, D.M. Marini, W. Hwang, S. Santoso, Design of nanostructured biological materials through self-assembly of peptides and proteins. Curr. Opin. Chem. Biol. **6**, 865–871 (2002). https://doi.org/10.1016/S1367-5931(02)00391-5
7. K. Rajagopal, J.P. Schneider, Self-assembling peptides and proteins for nanotechnological applications. Curr. Opin. Struct. Biol. **14**, 480–486 (2004). https://doi.org/10.1016/j.sbi.2004.06.006
8. E. Gazit, Self-assembled peptide nanostructures: the design of molecular building blocks and their technological utilization. Chem. Soc. Rev. **36**, 1263–1269 (2007). https://doi.org/10.1039/b605536m
9. X. Zhao, S. Zhang, Molecular designer self-assembling peptides. Chem. Soc. Rev. **35**, 1105–1110 (2006). https://doi.org/10.1039/b511336a
10. G. Chen, G.J. Mohamed, Complex protein patterns formation via salt-induced self-assembly and droplet evaporation. Eur. Phys. J. E **33**, 19–26 (2010). https://doi.org/10.1140/epje/i2010-10649-4
11. C. Tang, R.V. Ulijn, A. Saiani, Self-assembly and gelation properties of glycine/leucine Fmoc-dipeptides. Eur. Phys. J. E **36**, 111 (2013). https://doi.org/10.1140/epje/i2013-13111-3
12. Q. Zhang, M. Li, C. Zhu, G. Nurumbetov, Z. Li, P. Wilson, K. Kempe, D.M. Haddleton, Well-defined protein/peptide-polymer conjugates by aqueous Cu-LRP: synthesis and controlled self-assembly. J. Am. Chem. Soc. **137**, 9344–9353 (2015). https://doi.org/10.1021/jacs.5b04139
13. C.J.C. Edwards-Gayle, I.W. Hamley, Self-assembly of bioactive peptides, peptide conjugates, and peptide mimetic materials. Org. Biomol. Chem. **15**, 5867–5876 (2017). https://doi.org/10.1039/c7ob01092c
14. Z. Yang, H. Xu, X. Zhao, Designer self-assembling peptide hydrogels to engineer 3d cell microenvironments for cell constructs formation and precise oncology remodeling in ovarian cancer. Adv. Sci. **7**, 1903718 (2020). https://doi.org/10.1002/advs.201903718
15. J. Wang, J.Q.M. Choi, A.S. Holehouse, H.O. Lee, X. Zhang, M. Jahnel, S. Maharana, R. Lemaitre, A. Pozniakovsky, D. Drechsel, I. Poser, R.V. Pappu, S. Alberti, A.A. Hyman, A molecular grammar governing the driving forces for phase separation of prion-like rna binding proteins. Cell **174**, 688–699 (2018). https://doi.org/10.1016/j.cell.2018.06.006
16. A.A. Hyman, C.A. Weber, F. Jülicher, Liquid-liquid phase separation in biology. Annu. Rev. Cell Dev. Biol. **30**, 39–58 (2014). https://doi.org/10.1146/annurev-cellbio-100913-013325
17. C.P. Brangwynne, C.R. Eckmann, D.S. Courson, A. Rybarska, C. Hoege, J. Gharakhani, F. Jülicher, A.A. Hyman, Germline p granules are liquid droplets that localize by controlled dissolution/condensation. Science **324**, 1729–1732 (2009). https://doi.org/10.1126/science.1172046
18. Y. Lin, D.S.W. Protter, M.K. Rosen, R. Parker, Formation and maturation of phase-separated liquid droplets by rna-binding proteins. Mol. Cell **60**, 208–219 (2015). https://doi.org/10.1016/j.molcel.2015.08.018
19. T. Murakami, S. Qamar, J.Q. Lin, G.S.K. Schierle, E. Rees, A. Miyashita, A.R. Costa, R.B. Dodd, F.T.S. Chan, C.H. Michel, D. Kronenberg-Versteeg, Y. Li, S.Q.P. Yang, Y. Wakutani, W. Meadows, R.R. Ferry, L. Dong, G.G. Tartaglia, G. Favrin, W.Q.L. Lin, D.W. Dickson, M. Zhen, D. Ron, G. Schmitt-Ulms, P.E. Fraser, N.A. Shneider, C. Holt, M. Vendruscolo, C.F. Kaminski, P.S. George-Hyslop, Als/ftd mutation-induced phase transition of fus liquid droplets and reversible hydrogels into irreversible hydrogels impairs rnp granule function. Neuron **88**, 678–690 (2015). https://doi.org/10.1016/j.neuron.2015.10.030

20. D.T. Murray, M. Kato, Y. Lin, K.R. Thurber, I. Hung, S.L. McKnight, R. Tycko, Structure of fus protein fibrils and its relevance to self-assembly and phase separation of low-complexity domains. Cell **171**, 615–627 (2017). https://doi.org/10.1016/j.cell.2017.08.048
21. A. Patel, H.O. Lee, L. Jawerth, S. Maharana, M. Jahnel, M.Y. Hein, S. Stoynov, J. Mahamid, S. Saha, T.M. Franzmann, A. Pozniakovski, I. Poser, N. Maghelli, L.A. Royer, M. Weigert, E.W. Myers, S. Grill, D. Drechsel, A.A. Hyman, S. Alberti, A liquid-to-solid phase transition of the als protein fus accelerated by disease mutation. Cell **162**, 1066–1077 (2015). https://doi.org/10.1016/j.cell.2015.07.047
22. S. Boeynaems, S. Alberti, N.L. Fawzi, T. Mittag, M. Polymenidou, F. Rousseau, J. Schymkowitz, J. Shorter, B. Wolozin, L.V.D. Bosch, P. Tompa, M. Fuxreiter, Protein phase separation: a new phase in cell biology. Trends Cell Biol. **28**, 420–435 (2018). https://doi.org/10.1016/j.tcb.2018.02.004
23. A. Molliex, J. Temirov, J. Lee, M. Coughlin, A.P. Kanagaraj, H.J. Kim, T. Mittag, J.P. Taylor, Phase separation by low complexity domains promotes stress granule assembly and drives pathological fibrillization. Cell **163**, 123–133 (2015). https://doi.org/10.1016/j.cell.2015.09.015
24. K.A. Burke, A.M. Janke, C.L. Rhine, N.L. Fawzi, Residue-by-residue view of in vitro fus granules that bind the c-terminal domain of rna polymerase ii. Mol. Cell **60**, 231–241 (2015). https://doi.org/10.1016/j.molcel.2015.09.006
25. Z. Feng, X. Chen, X. Wu, M. Zhang, Formation of biological condensates via phase separation: characteristics, analytical methods, and physiological implications. J. Biol. Chem. **294**, 14823–14835 (2019). https://doi.org/10.1074/jbc.REV119.007895
26. C.W. Pak, M. Kosno, A.S. Holehouse, S.B. Padrick, A. Mittal, R. Ali, A.A. Yunus, D.R. Liu, R.V. Pappu, M.K. Rosen, Sequence determinants of intracellular phase separation by complex coacervation of a disordered protein. Mol. Cell **63**, 72–85 (2016). https://doi.org/10.1016/j.molcel.2016.05.042
27. G.L. Dignon, W. Zheng, Y.C. Kim, J. Mittal, Temperature-controlled liquid-liquid phase separation of disordered proteins. ACS Cent. Sci. **5**, 821–830 (2019). https://doi.org/10.1021/acscentsci.9b00102
28. S. Alberti, D. Dormann, Liquid-liquid phase separation in disease. Annu. Rev. Genet. **53**, 171–194 (2019). https://doi.org/10.1146/annurev-genet-112618-043527
29. A. Peng, S.C. Weber, Evidence for and against liquid-liquid phase separation in the nucleus. Non-Coding RNA **5**, 50 (2019). https://doi.org/10.3390/ncrna5040050
30. F.G. Quiroz, N.K. Li, S. Roberts, P. Weber, M. Dzuricky, I. Weitzhandler, Y.G. Yingling, A. Chilkoti, Intrinsically disordered proteins access a range of hysteretic phase separation behaviors. Sci. Adv. **5**, 5177 (2019). https://doi.org/10.1126/sciadv.aax5177
31. B.S. Schuster, E.H. Reed, R. Parthasarathy, C.N. Jahnke, R.M. Caldwell, J.G. Bermudez, H. Ramage, M.C. Good, D.A. Hammer, Controllable protein phase separation and modular recruitment to form responsive membraneless organelles. Nat. Commun. **9**, 2985 (2018). https://doi.org/10.1038/s41467-018-05403-1
32. I.E. Vega, A. Umstead, N.M. Kanaan, Efhd2 affects tau liquid-liquid phase separation. Front. Neurosci. **13**, 845 (2019). https://doi.org/10.3389/fnins.2019.00845
33. Q. Li, X. Peng, Y. Li, W. Tang, J. Zhu, J. Huang, Y. Qi, Z. Zhang, Llpsdb: A database of proteins undergoing liquid-liquid phase separation In Vitro. Nucleic Acids Res. (2019). https://doi.org/10.1093/nar/gkz778
34. O. Adame-Arana, C.A. Weber, V. Zaburdaev, J. Prost, F. Jülicher, Liquid phase separation controlled by ph. Biophys. J . **119**, 1590–1605 (2020). https://doi.org/10.1016/j.bpj.2020.07.044
35. G. Krainer, T.J. Welsh, J.A. Joseph, J.R. Espinosa, S. Wittmann, E. Csilléry, A. Sridhar, Z. Toprakcioglu, G. Gudiškytė1, M.A. Czekalska, W.E. Arter, J. Guillén-Boixet, T.M. Franzmann, S. Qamar, P.S. George-Hyslop, A.A. Hyman, R. Collepardo-Guevara, S. Alberti, T.P.J. Knowles, Reentrant liquid condensate phase of proteins is stabilized by hydrophobic and non-ionic interactions. Nat. Commun. **12**, 1085 (2021). https://doi.org/10.1038/s41467-021-21181-9
36. S. Zhang, L. Yan, M. Altman, M. Lässle, H. Nugent, F. Frankel, D.A. Lauffenburger, G.M. Whitesides, A. Rich, Biological surface engineering: a simple system for cell pattern formation. Biomaterials **20**, 1213–1220 (1999). https://doi.org/10.1016/S0142-9612(99)00014-9
37. Y.Q.P. Jiao, F.Q.Z. Cui, Surface modification of polyester biomaterials for tissue engineering. Biomed. Mater. **2**, 24–37 (2007). https://doi.org/10.1088/1748-6041/2/4/R02
38. S. Nir, D. Zanuy, T. Zada, O. Agazani, C. Aleman, D.E. Shalev, M. Reches, Tailoring the self-assembly of a tripeptide for the formation of antimicrobial surfaces. Nanoscale **11**, 8752–8759 (2019). https://doi.org/10.1039/C8NR10043H
39. S. Zhang, T.C. Holmes, C.M. DiPersio, R.O. Hynes, X. Su, A. Rich, Self-complementary oligopeptide matrices support mammalian cell attachment. Biomaterials **16**, 1385–1393 (1995). https://doi.org/10.1016/0142-9612(95)96874-Y
40. E.C. Wu, S. Zhang, C.A.E. Hauser, Self-assembling peptides as cell-interactive scaffolds. Adv. Funct. Mater. **22**, 456–468 (2012). https://doi.org/10.1002/adfm.201101905
41. L. Sun, C. Zheng, T.J. Webster, Self-assembled peptide nanomaterials for biomedical applications: promises and pitfalls. Int. J. Nanomedicine **12**, 73–86 (2017). https://doi.org/10.2147/IJN.S117501
42. S. Zhang, Fabrication of novel biomaterials through molecular self-assembly. Nat. Biotechnol. **21**, 1171–1178 (2003). https://doi.org/10.1038/nbt874
43. L. Adler-Abramovich, E. Gazit, The physical properties of supramolecular peptide assemblies: from building block association to technological applications. Chem. Soc. Rev. **43**, 6881–6893 (2014). https://doi.org/10.1039/c4cs00164h
44. D.M. Shapiro, G. Mandava, S.E. Yalcin, P. Arranz-Gibert, P.J. Dah, C. Shipps, Y. Gu, V. Srikanth, A.I. Salazar-Morales, J.P. ÓBrien, K. Vanderschuren, D. Vu, V.S. Batista, N.S. Malvankar, F.J. Isaacs, Protein nanowires with tunable functionality and programmable self-assembly using sequence-controlled synthesis. Nat. Commun. **13**, 829 (2022). https://doi.org/10.1038/s41467-022-28206-x

45. R.W. Carrell, B. Gooptu, Conformational changes and disease-serpins, prions and Alzheimer's. Curr. Opin. Struct. Biol. **8**, 799–809 (1998). https://doi.org/10.1016/S0959-440X(98)80101-2
46. C. Soto, G.P. Saborío, Prions: Disease propagation and disease therapy by conformational transmission. Trends Mol. Med. **7**, 109–114 (2001). https://doi.org/10.1016/S1471-4914(01)01931-1
47. S.T. Ferreira, F.G. De Felice, Protein dynamics, folding and misfolding: from basic physical chemistry to human conformational diseases. FEBS Lett. **498**, 129–134 (2001). https://doi.org/10.1016/S0014-5793(01)02491-7
48. E. Žerovnik, Amyloid-fibril formation: proposed mechanisms and relevance to conformational disease. Eur. J. Biochem. **269**, 3362–3371 (2002). https://doi.org/10.1046/j.1432-1033.2002.03024.x
49. N. Ghoshal, F. García-Sierra, J. Wuu, S. Leurgans, D.A. Bennett, R.W. Berry, L.I. Binder, Tau conformational changes correspond to impairments of episodic memory in mild cognitive impairment and Alzheimer's disease. Exp. Neurol. **177**, 475–493 (2002). https://doi.org/10.1006/exnr.2002.8014
50. E. Gazit, Mechanisms of amyloid fibril self-assembly and inhibition: model short peptides as a key research tool. FEBS J. **272**, 5971–5978 (2005). https://doi.org/10.1111/j.1742-4658.2005.05022.x
51. S. Lee, T.H.T. Trinh, M. Yoo, J. Shin, H. Lee, J. Kim, E. Hwang, Y.-B. Lim, C. Ryou, Self-assembling peptides and their application in the treatment of diseases. Int. J. Mol. Sci. **20**, 5850 (2019). https://doi.org/10.3390/ijms20235850
52. H. Yang, S.Q.Y. Fung, M. Pritzker, P. Chen, Modification of hydrophilic and hydrophobic surfaces using an ionic-complementary peptide. PLoS ONE **2**, 1325 (2007). https://doi.org/10.1371/journal.pone.0001325
53. M. Stefani, Protein folding and misfolding on surfaces. Int. J. Mol. Sci. **9**, 2515–2542 (2008). https://doi.org/10.3390/ijms9122515
54. S. Jun, Y. Hong, H. Imamura, B.Q.Y. Ha, J. Bechhoefer, P. Chen, Self-assembly of the ionic peptide EAK16: the effect of charge distributions on self-assembly. Biophys. J . **87**, 1249–1259 (2004). https://doi.org/10.1529/biophysj.103.038166
55. M. Reches, E. Gazit, Controlled patterning of aligned self-assembled peptide nanotubes. Nat. Nanotechnol. **1**, 195–200 (2006). https://doi.org/10.1038/nnano.2006.139
56. Y.Q.C. Lin, E.J. Petersson, Z. Fakhraai, Surface effects mediate self-assembly of Amyloid-β peptides. ACS Nano **8**, 10178–10186 (2014). https://doi.org/10.1021/nn5031669
57. S. Emamyari, H. Fazli, pH-dependent self-assembly of EAK16 peptides in the presence of a hydrophobic surface: Coarse-grained molecular dynamics simulation. Soft Matter **10**, 4248–4257 (2014). https://doi.org/10.1039/c4sm00307a
58. S. Emamyari, F. Kargar, V. Sheikh-hasani, S. Emadi, H. Fazli, Mechanisms of the self-assembly of EAK16-family peptides into fibrillar and globular structures: molecular dynamics simulations from nano- to micro-seconds. Eur. Biophys. J. **44**, 263–276 (2015). https://doi.org/10.1007/s00249-015-1024-y
59. B. Yang, D.J. Adams, M. Marlow, M. Zelzer, Surface-mediated supramolecular self-assembly of protein, peptide, and nucleoside derivatives: from surface design to the underlying mechanism and tailored functions. Langmuir **34**, 15109–15125 (2018). https://doi.org/10.1021/acs.langmuir.8b01165
60. D. Wouters, U.S. Schubert, Nanolithography and nanochemistry: Probe-related patterning techniques and chemical modification for nanometer-sized devices. Angew. Chem. Int. Ed. **43**, 2480–2495 (2004). https://doi.org/10.1002/anie.200300609
61. C.J. Bowerman, B.L. Nilsson, Self-assembly of amphipathic β-sheet peptides: insights and applications. Biopolymers (Pept. Sci.) **98**, 169–184 (2012). https://doi.org/10.1002/bip.22058
62. M. Rubinstein, R.H. Colby, *Polymer Physics*, 1st edn. (Oxford University Press, New York, 2003)
63. F. Huang, W.M. Nau, A conformational flexibility scale for amino acids in peptides. Angew. Chem. Int. Ed. **42**, 2269–2272 (2003). https://doi.org/10.1002/anie.200250684
64. S. Rekhi, D.S. Devarajan, M.P. Howard, Y.C. Kim, A. Nikoubashman, J. Mittal, Role of strong localized vs weak distributed interactions in disordered protein phase separation. J. Phys. Chem. B **127**(17), 3829–3838 (2023). https://doi.org/10.1021/acs.jpcb.3c00830
65. F. Weik, R. Weeber, K. Szuttor, K. Breitsprecher, J. Graaf, M. Kuron, J. Landsgesell, H. Menke, D. Sean, C. Holm, Espresso 4.0 - an extensible software package for simulating soft matter systems. Eur. Phys. J.: Spec. Top. **227**, 1789–1816 (2019). https://doi.org/10.1140/epjst/e2019-800186-9
66. A.P. Thompson, H.M. Aktulga, R. Berger, D.S. Bolintineanu, W.M. Brown, P.S. Crozier, P.J. Veld, A. Kohlmeyer, S.G. Moore, T.D. Nguyen, R. Shan, M.J. Stevens, J. Tranchida, C. Trott, S.J. Plimpton, Lammps - a flexible simulation tool for particle-based materials modeling at the atomic, meso, and continuum scales. Comp. Phys. Comm. **271**, 108171 (2022). https://doi.org/10.1016/j.cpc.2021.108171
67. M.K. Singh, M. Hu, Y. Cang, H.P. Hsu, H. Therien-Aubin, K. Koynov, G. Fytas, K. Landfester, K. Kremer, Glass transition of disentangled and entangled polymer melts: single-chain-nanoparticles approach. Macromolecules **53**(17), 7312–7321 (2020). https://doi.org/10.1021/acs.macromol.0c00550
68. K.S. Silmore, M.P. Howard, A.Z. Panagiotopoulos, Vapour-liquid phase equilibrium and surface tension of fully flexible lennard-jones chains. Mol. Phys. **115**(3), 320–327 (2017). https://doi.org/10.1080/00268976.2016.1262075